PCCP

Accepted Manuscript

ROYAL SOCIETY OF CHEMISTRY

www.rsc.org/pccp

PCCP

RSCPublishing

PAPER

Fine tunable aqueous solution synthesis of textured flexible SnS_2 thin films and nanosheets

Cite this: DOI: 10.1039/x0xx00000x

Peter Nørby,[†] Simon Johnsen,[†] and Bo Brummerstedt Iversen*

Received 00th January 2012,
Accepted 00th January 2012

DOI: 10.1039/x0xx00000x

www.rsc.org/pccp

Films and nanosheets of layered chalcogenides are currently under intense investigation owing to their application in thin film electronic, optoelectronic, and sensor devices. Here, aqueous solution processing of the environmentally benign thiostannate, $(NH_4)_4Sn_2S_6{\cdot}3H_2O$, and its subsequent thermal decomposition to form continuous highly textured SnS_2 thin films are presented. We show how to control the film thickness, the coherent scattering domain size, and the crystallinity by changes in the processing parameters (*i.e.* thiostannate concentration or angular velocity in the spin coating process). For device applications of the semiconducting metal sulfide film it is of interest to delaminate the film from the glass substrate to create freestanding nanosheets or transfer the film to a flexible polymer substrate. It is shown how metal sulfide films can be delaminated from the glass substrate and form large area freestanding nanosheets. Furthermore, we extend the delamination process to include transfer of the thin film from the glass substrate to a low-cost flexible polymer substrate.

1 Introduction

High mobility semiconducting thin films form the basis of a wealth of electronic, optoelectronic, and sensing devices that surround us in everyday life. Nanosheets of graphene-like metal chalcogenides are emerging as a new material class within these applications.[1–5] Often, nanosheets of these layered chalcogenides are produced using either mechanically or chemically exfoliated layers.[6,7] Other methods include sulfurization of evaporated metal layers,[8,9] chemical vapor deposition,[9–11] and thermal decomposition of dip coated layers.[12] SnS_2 has attracted significantly less attention than the transition metal chalcogenide counterparts such as MoS_2 and WS_2. Nevertheless, exfoliated multilayers of SnS_2 have been integrated into thin film transistor (TFT) devices with carrier mobilities of up to ~50 $cm^2V^{-1}s^{-1}$.[13–15] While exfoliation, sulfurization of metal layers, and similar methods yield remarkable results they are challenging to integrate into a manufacturing process. Solution processing is particularly attractive from a fabrication point of view since deposition equipment is low-cost and compatible with high throughput methods such as roll-to-roll processing or different types of printing. Laboratory devices of both SnS_2 and SnS_2-based multinary films, fabricated using solutions or colloids, have shown performances matching or and even exceeding established industrial device techniques, but at a promise of greatly reduced processing costs.[16–20]
Thin film of SnS_2 has been chemical solution deposited either by the successive ionic layer adsorption and reaction (SILAR) technique[21] or dip coating.[22] Recently, the use of the solution processing technique on all-inorganic solutions,[16,23–27] suspensions,[20,28,29] or slurries[30] have emerged as an effective approach to achieve superior device performances. High mobility multinary SnS_2-based films fabricated using all-inorganic solutions performed extraordinarily well in TFTs and the method is applicable to a wide range of metal chalcogenide systems.[26,27,31] Hydrazine has been the long-term favorite solvent in solution processing of metal chalcogenide systems owing to its high solubility of many metal chalcogenides.[27,32] However, use of the highly toxic and flammable hydrazine as a solvent is problematic for industrial processing.[32] Here we present the synthesis of highly textured SnS_2 thin films by thermal decomposition of aqueous solution deposited ammonium thiostannate(IV), where the highly toxic/flammable hydrazine has been replaced by water. This is a significant step forward towards a more environmental friendly formation of SnS_2 thin films and SnS_2-based multinary phases. Moreover, we show how to fabricate large area freestanding nanosheets of the solution processed SnS_2 thin films by a delamination of the film from its glass substrate. Obvious applications for such metal sulfide nanosheets, apart from being the active layer in electronic devices, are in sensor and gas separation applications.[33,34] Metal chalcogenide based membranes have shown high gas selectivity, because of their large polarizability compared to *e.g.* the often used oxide materials.[35,36] Furthermore, SnS_2 has shown to have potential as a photocatalyst.[37,38]

Deposition of active layers on cheap, flexible, and transparent polymer substrates is attractive in the electronic, optoelectronic, and sensor applications. Though the process of transforming $(NH_4)_4Sn_2S_6$ solution to crystalline SnS_2 films occurs at temperatures as low as 220 °C, is it not compatible with many inexpensive polymer substrates. Here we show how to transfer the metal sulfide film from the glass substrate onto the inexpensive low temperature polymer, poly(methyl methacrylate) (PMMA). Hereby it is possible to reap the benefits of the glass substrate during the film formation and the advantages of the polymer substrate in the final device application.

2 Experimental

2.1 Preparation of aqueous solutions of $(NH_4)_4Sn_2S_6{\cdot}3H_2O$

The ammonium thiostannate(IV) solution was made by dissolving $(NH_4)_4Sn_2S_6{\cdot}3H_2O$ crystals in water. $(NH_4)_4Sn_2S_6{\cdot}3H_2O$ was synthesized as previously reported.[39] In a typical synthesis ~0.50 mmol of $(NH_4)_4Sn_2S_6{\cdot}3H_2O$ was dissolved in ~5 mL of MilliQ water to yield a clear solution with a concentration of ~0.25 M (based on the $[Sn_2S_6]^{4-}$ dimer). Because of NH_3 and H_2S gaseous losses the solution can turn opaque. Addition of two drops of aqueous $(NH_4)_2S$ solution (20 wt%) restores the clear solution. Alternatively, SnS_2 dissolved in aqueous $(NH_4)_2S$ can also be used as precursor solution (details in supporting information).

2.2 Thin film fabrication

The films are fabricated in an N_2 filled glove box using the above ammonium thiostannate(IV) solutions. Prior to deposition the substrate is cleaned using a 70-80 °C heated Micro-90® solution (1:4 with MilliQ water), rinsed in MilliQ water, and followed by three consecutive 10 minutes sonications (VWR, 45 kHz, 60 W) in MilliQ water. For a typical thin film fabrication a 0.25 M $(NH_4)_4Sn_2S_6{\cdot}3H_2O$ (thiostannate(IV)) solution is added to a 25x25 mm glass substrate (cut from Menzel-Gläser microscope slides) to cover the entire surface. The solution is passed through a Ø0.2 µm PTFE filter to avoid particle contamination. The substrate is spun at 2000 rpm (Laurell WS-650Mz-23NPP) and fresh $(NH_4)_4Sn_2S_6{\cdot}3H_2O$ solution is added during rotation, after which the wafer is left spinning for 120 s. Subsequently, it is transferred to a calibrated hot plate and heated to the desired decomposition/annealing temperature, where it rests for 300 s. The correlation between the hot plate set temperature and the actual annealing temperature on the glass substrate was calibrated by a thermocouple glued onto a glass substrate. The typical calibrated annealing temperature was 300 °C.

2.3 Thin film delamination

(Caution! Hydrofluoric acid is highly corrosive and skin penetrating. Handle with care and appropriate safety equipment.) The structure consisting of the metal sulfide thin film on-top of the SiO_2 based substrate is immersed in a 0.5 M aqueous HF solution. After 1h (for a 60 nm thick SnS_2 thin film) the delamination process is complete and a free-floating metal sulfide nanosheet is obtained.

2.4 Substrate transfer

The SnS_2 thin film (see above for synthesis details) is soaked in a 1 M aqueous HCl solution (filtered using Ø0.2 µm PTFE filter) for 10 s, then spun at 3000 rpm/60 s, and heated to 90 °C for 180 s. Then dodecanethiol (≥98%, Sigma-Aldrich) is deposited on the SnS_2 thin film (filtered using Ø0.2 µm PTFE filter), left for 10 s, then spun at 3000 rpm/60 s and annealed at 180°C/90 s. Finally a 20 µm thick PMMA layer (see supporting information) is deposited on top of the 60 nm thick SnS_2 thin film using spin coating. PMMA (average M_w ~ 120.000 $g{\cdot}mol^{-1}$, Sigma-Aldrich) is dissolved in chlorobenzene (ACS reagent, Sigma-Aldrich) to yield a 10 wt% solution. The film was spun at 1000 rpm/60 s and annealed at 180°C/90 s. 5 additional layers were deposited on top of the as-spin coated film using a commercial airbrush, 15 cm above the film. The solution was deposited on the cold structure, which was annealed at 180°C/90 s between coatings. The delamination process is identical to the process for the bare metal chalcogenide film except for a longer immersion time of 24 h. To avoid bending of the PMMA it can be mounted on a rigid polystyrene substrate using double-sided adhesive tape prior to delamination.

2.5 Film characterization

X-ray reflectivity (XRR) was measured in the 2θ-range from 0-3° on a Rigaku SMARTlab equipped with a rotating Cu anode (λ = 1.54056 Å) and parallel beam optics, which also was used to measure X-ray diffraction (XRD) in reflection geometry. Transmission electron microscope photographs of the delaminated films were recorded using a Phillips Model CM20 TEM microscope working at 200 kV.

3 Results and Discussion

In aqueous ammonium sulfide solution, SnS_2 dissolves to form the complex $(NH_4)_4Sn_2S_6$.[39,40] From these aqueous ammonium thiostannate(IV) solutions we have recently reported the crystallization of $(NH_4)_4Sn_2S_6{\cdot}3H_2O$.[39] Spin coating of $(NH_4)_4Sn_2S_6$ solution and subsequent thermal decomposition permits deposition of a SnS_2 layer. The initial layer formed is transparent/white opaque in appearance, which under mild heating transforms to a yellow layer. This consist presumably of a condensed amorphous composition including $[Sn_4S_{10}]^{4-}$ units as reported earlier.[39] Further heating results in complete decomposition and formation of a SnS_2 film through the total reaction in the following equation:

$$(NH_4)_4Sn_2S_6(aq) + \Delta \rightarrow 2SnS_2(s) + 2H_2S(g) + 4NH_3(g)$$

Fig. 1 shows XRD patterns of SnS_2 films on glass substrates. The patterns show a pronounced preferential orientation with the [001] direction perpendicular to the

substrate surface, which was also observed for SnS_2 thin films processed from $(N_2H_5)_4Sn_2S_6$ hydrazine solution.[27] Since the in-plane electron mobility (plane spanned by the [100] and [010] vectors) is significantly higher than the out-of-plane,[41] this promotes a high mobility film suited for *e.g.* TFTs. To establish the annealing temperature effect on the grain size, ~700 nm thick films were deposited using a slow angular spin velocity (750 rpm) and high precursor thiostannate(IV) concentration (0.375 M). Thick films are used to avoid that crystallite sizes are limited by the film thickness.

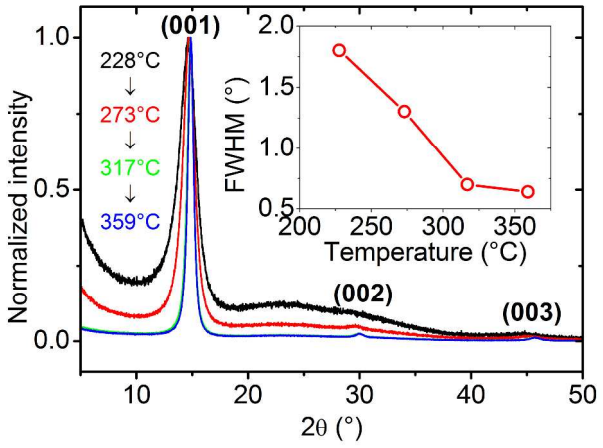

Fig. 1. XRD pattern of SnS_2 films (~700 nm) annealed at four different temperatures (228 °C, 273 °C, 317 °C, and 359 °C). Inset shows the FWHM for the (001) peak as a function of annealing temperature.

The annealing temperature dependence on the full width at half maximum (FWHM) is shown in the inset of Fig. 1. There is a pronounced reduction of the FWHM for the peak as the annealing temperature increases. This translates into a size increase in the coherent scattering domains along [001] from 5 nm at 228 °C to 12 nm at 359 °C (Fig. S2) using the Scherrer equation under the assumption of spherical crystallites. However, non-uniform strain and stacking faults are likely to contribute to the peak broadening. Also the crystallinity is significantly increased as evidenced by the absence of the amorphous background for the higher annealing temperatures. Hence, processing is possible at temperatures compatible with polymer substrates such as polyimide. However, there are benefits in terms of increased crystallinity and increases in the coherent scattering domains (grain growth, loss of strain and stacking faults) with annealing at temperatures solely compatible with inorganic substrates.

The X-ray reflectivity (XRR) datasets of thin films synthesized (thiostannate(IV) concentration 0.25 M) using variable angular velocity in the spin coating process and then annealed at 300 °C show the Kiessig fringes typical for a thin film with a homogeneous thickness, Fig. 2. The critical angle is $\theta_c \sim 0.28°$, which translates into an average density of ~4 $g \cdot cm^{-3}$ assuming SnS_2 composition. In refinements of the XRR data (see supporting information for details) a linear density gradient was used going from the top to the substrate side. From the model refinements the thickness of the films was extracted and typical results are shown in the insert of Fig. 2. It is evident that the thickness of the synthesized thin films can be varied by adjusting the angular velocity of the spin coater. Similarly, through tuning of the thiostannate(IV) concentration the film thickness can be varied *e.g.* changing the concentration from 0.25 M to 0.15 M reduces the final SnS_2 film thickness from 70 nm to 43 nm (angular velocity 2000 rpm and annealing at 300 °C; see supporting information for details). Hence, it is possible to fine-tune the thickness of the films formed by adjusting either the angular spin velocity or the thiostannate(IV) concentration.

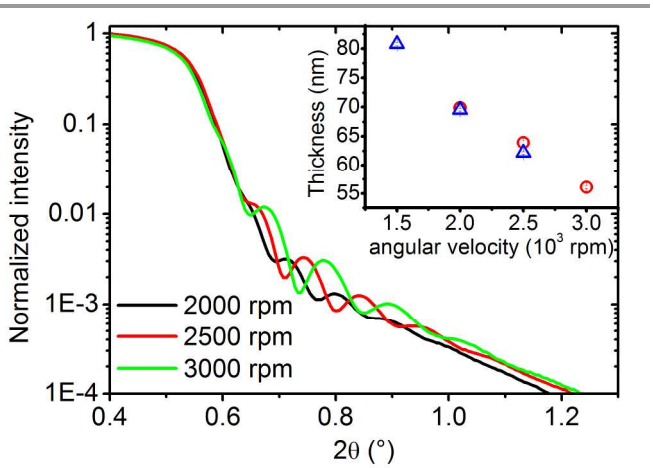

Fig. 2. X-ray reflectivity data of samples spin coated at different angular velocities and annealed at 300 °C. (Inset) Thickness of SnS_2 film as obtained by refinement of X-ray reflectivity data (see supporting information for details). The data points marked by red circles are refined to the X-ray reflectivity data shown in the main figure, while the blue triangles are refined thicknesses from an independent synthesis series.

Solution deposited metal sulfide thin films can be useful directly on a high temperature substrate *e.g.* in a thin film transistor structure.[26,27,32] However, in applications as *e.g.* nanomembranes or nanosheet sensors freestanding films are useful.[42] For delamination of the thin films from the glass substrate we utilized the fact that several metal sulfides *e.g.* SnS_2 do not dissolve in diluted acids. HF on the other hand readily dissolves SiO_2. Hence, by exposing the metal chalcogenide/glass structure to a dilute HF solution, bonds to the SiO_2 based substrate are cleaved and the continuous film is delaminated from the substrate, Fig. 3. Complete delamination of a ~1 cm^2 66(1) nm film occurs within ~1 hour. The process proceeds both from the edges and possibly also through diffusion of HF through the thin SnS_2 layer. The latter effect is evidenced by the longer delamination time of a SnS_2/PMMA structure from the glass substrate, where only the edges are exposed. Fig. 4 shows a ~1 cm^2 delaminated SnS_2 film only 66(1) nm thick floating in 0.5 M aqueous HF.

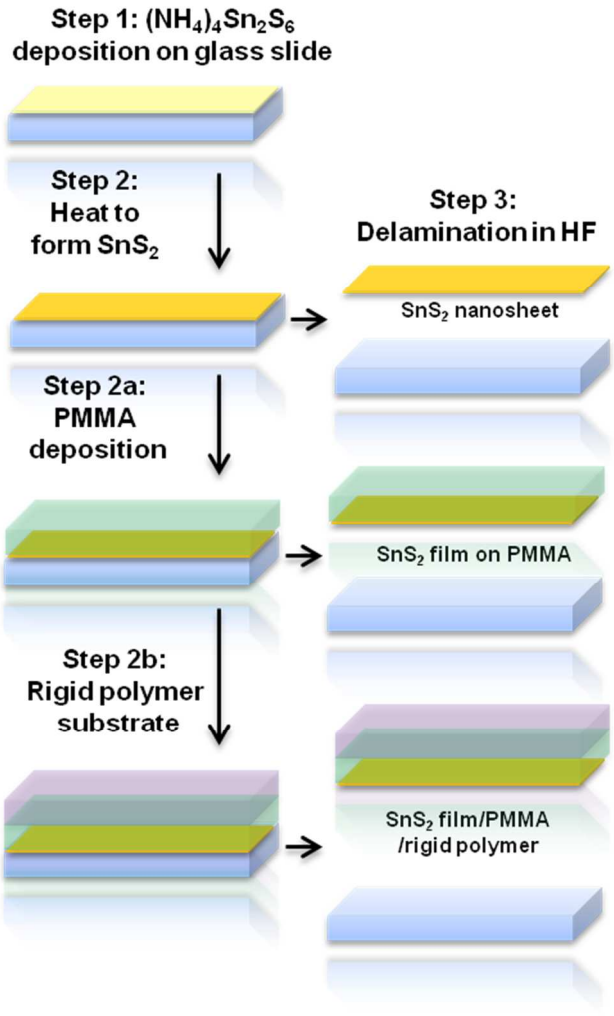

Fig. 3. Schematic of the steps in the delamination and substrate transfer of the SnS_2 film.

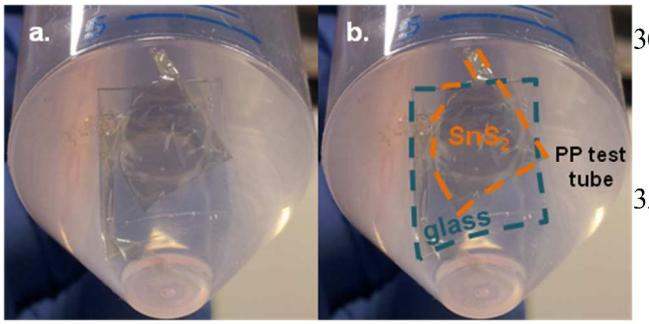

Fig. 4. a) Photograph of a delaminated 66(1) nm yellow transparent SnS_2 thin film floating in 0.5 M aqueous HF beside the stripped glass slide in a polypropylene (PP) test tube. b) Photograph in a) with the thin film and glass substrate edges outlined by dashed lines.

TEM investigation (Fig. 5) of the delaminated film shows that within the resolution of the microscope the film is continuous without pores extending through it.[39] The edge of the film shows nanoparticles in the sub-20 nm regime,[39] in good agreement with the crystallite sizes found by (001) peak broadening via the Scherrer equation. The continuity of the film is obviously important for applications in electronic devices, where the mobility of the charge carriers is adversely affected by porosity and non-continuity. Coupled with the attractive texture found above in the XRD study, good electronic properties of the films can be expected.

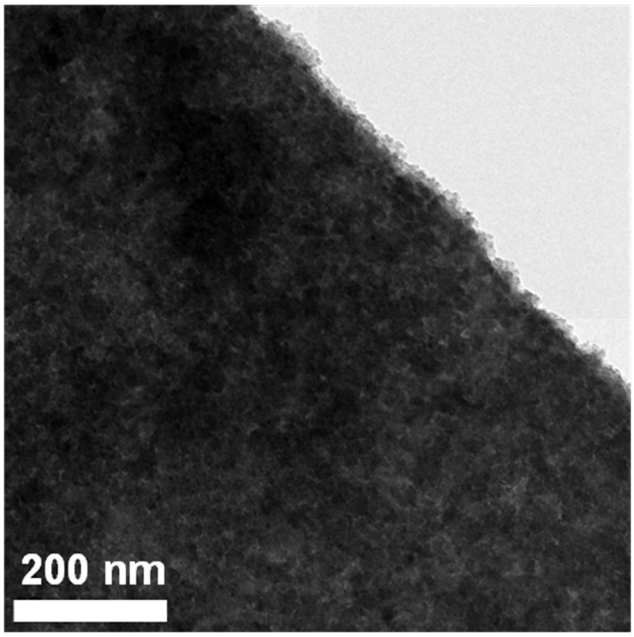

Fig. 5. TEM photograph of a 60(5) nm thick delaminated SnS_2 nanosheet.

Substrate transfer from the high temperature glass substrates to low temperature polymer substrates is potentially very important for the production of high mobility flexible electronics, optoelectronics, or sensor devices. Substrate transfer is often performed using a polymeric sacrificial layer, which is deposited on-top of a rigid substrate (typically glass or Si wafer). The inorganic thin film is now deposited on top of this sacrificial layer and the new substrate (typically polymeric) is solution processed to form a substrate/sacrificial layer/active layer/new substrate structure. However the use of polymers severely limits the maximum annealing temperature of the substrate. Consequently, the inorganic active layer cannot be annealed at sufficiently high temperature to ensure optimal performance. As previously pointed out, the crystallinity of the metal sulfide film markedly increases with increasing annealing temperature. The lowest annealing temperature presented here is compatible with *e.g.* polyimide polymeric substrates, but not compatible with cheaper substrates such as polyethylene terephthalate (PET) or PMMA. No polymer substrates can withstand the higher annealing temperatures, which are crucial in forming fully crystalline films. Furthermore, the chemical bonding between a polymeric sacrificial layer and the inorganic active layer can be challenging and result in imperfect film formation. Delamination methods solely involving high temperature substrates have been developed and *e.g.* MoS_2 grown on alumina substrates can be delaminated using NaOH etching.[10,12] SnS_2, however, dissolves in alkaline solutions.

Similarly, protecting layers are often applied to avoid degradation of the active film in the delamination process. This obviously leads to additional complication in the fabrication process. The method presented below involves a very temperature stable and chemical robust sacrificial layer, *i.e.* a glass slide. No protecting layers are needed in this method.

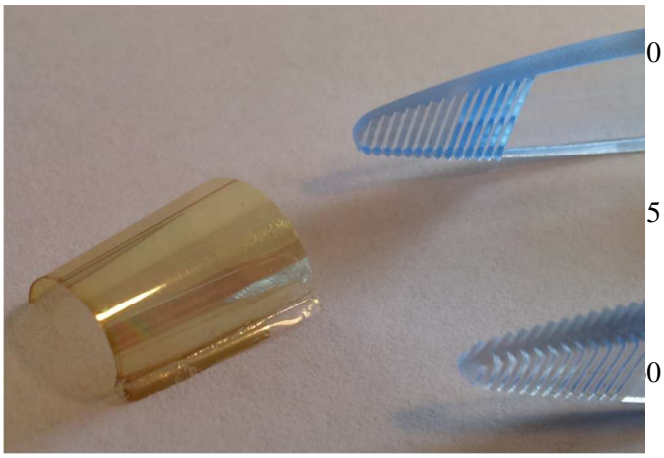

Fig. 6. 12x12 mm^2 SnS_2 film on the PMMA substrate after substrate transfer

Synthesis of the active film on the chemically and thermally robust SiO_2 allows deposition of higher quality thin films because: 1) The maximum annealing temperature of the substrate is not limited by a polymer but by the glass itself *i.e.* the solution processed films can be annealed at higher temperatures. 2) The glass substrate is insensitive to the harsh chemical environment present during the solution processing and thermal decomposition. 3) The inorganic glass surface is chemically compatible with the inorganic active layer. Provided the SnS_2 films can easily be transferred to polymer substrates, flexible devices with a metal sulfide active layer can be produced. PMMA was chosen because it is easily processable and resistant to dilute hydrofluoric acids.[43] Fig. 6 shows a SnS_2 thin film on PMMA after the delamination from the glass substrate. Note, the SnS_2 thin film has been inverted in this process and the bottom SnS_2 layer on the glass substrate is now at the SnS_2/air interface. We have shown that the porosity increases towards the surface, when the SnS_2 thin film is annealed on glass substrates.[39] Hence, the substrate transfer procedure presented here most likely reduces the thin film surface porosity.

We found that the thin film to PMMA adherence could be increased by first treating the SnS_2 thin film with 1 M HCl followed by a dodecanethiol treatment before the PMMA deposition. Likely the first step strips the SnS_2 surface of S atoms, which then facilitates the dodecanethiol bonding to the surface. The dodecanethiol in turn increases the adherence of PMMA on the SnS_2 by rendering the SnS_2 surface hydrophobic with long aliphatic hydrocarbon chains attached. After the substrate transfer the sample spontaneously bends (~180° over 12 mm) presumably because of strain induced in the thick PMMA layer during the solution deposition. In order to measure XRD on the sample after substrate transfer we taped the PMMA/SnS_2 structure to a flat substrate holder. The sample retains its texture during the substrate transfer (Fig. 7), but the appearance of the (011) peak (or the (111) which coincides with (011) in 2θ) suggests adverse effects of the dramatic bending of the PMMA/SnS_2 structure as result of both the PMMA layer strain, which bends the structure ~180° over the 12 mm width, as well as the following re-flattening of the structure when the XRD is performed. Prior to delamination of the glass/SnS_2/PMMA structure, it can be adhered to a semi-rigid polystyrene substrate using double sided adhesive tape on the PMMA side (Fig. 3 step 2b). Delamination now results in the rigid structure SnS_2/PMMA/tape/polystyrene, which eliminates the bending because of strain in the PMMA layer. Consequently, the texture is completely retained in this structure configuration and it confirms that the appearance of the additional Bragg peaks is a result of the dramatic bending. Slight bending of the semi-rigid polystyrene does not induce delamination of SnS_2 from the PMMA. Clearly, this is important for device applications where the integrity of the film is important.

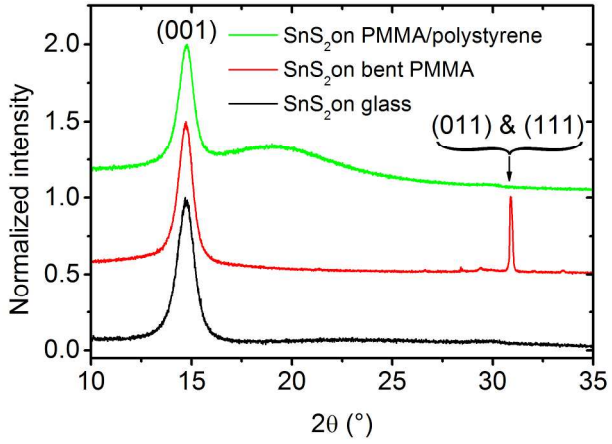

Fig. 7. Reflection mode diffraction patterns of SnS_2 films on different substrates.

4 Conclusion

We have shown how to prepare textured semiconducting SnS_2 thin films on glass substrates by spin coating of aqueous $(NH_4)_4Sn_2S_6$ solutions, which represents a safe and green alternative to the hydrazine solvent typically used. The layers are continuous and of homogeneous thickness. The latter can be controlled by tuning the thiostannate(IV) concentration and/or the angular velocity in the spin coating process. Furthermore, we have shown how to delaminate large area freestanding nanosheets of SnS_2 from their glass substrate, which could be useful in *e.g.* sensor or membrane applications. Delamination methods often include polymeric sacrificial and protecting layers which either limit the thermal treatment of the structure or complicate the delamination process, but in the present method there is no need for such layers. Consequently, the process is simple and the annealing temperature is limited by the glass substrate, which permits high temperature annealing to achieve highly crystalline films. Moreover, we have shown

how to transfer the high temperature annealed semiconducting thin film onto a flexible low cost polymer. Such a substrate transfer process could be an important step in the integration of high performance solution processed active layers in flexible devices. The method can be extended to delaminate several other metal chalcogenide thin films from their SiO_2 based substrates *e.g.* the layered MoS_2 and WS_2.

Acknowledgements

The Villum Foundation and the Danish National Research Foundation (Center for Materials Crystallography, DNRF93) are thanked for financial support. The authors declare no competing financial interest.

Notes and references

Center for Materials Crystallography (CMC) at Department of Chemistry and iNANO, Aarhus University, Langelandsgade 140, DK-8000 Aarhus C, Denmark
E-mail: bo@chem.au.dk
† These authors contributed equally to this work.

Electronic Supplementary Information (ESI) available: Experimental details on thin film synthesis, scotch tape test of the thin films, calculation of size of coherent scattering domains using XRD peak broadening, determination of PMMA thickness and details of XRR data fitting. See DOI: 10.1039/b000000x/

1 M. Chhowalla, H. S. Shin, G. Eda, L.-J. Li, K. P. Loh and H. Zhang, *Nat. Chem.*, 2013, **5**, 263–75.
2 X. Huang, Z. Zeng and H. Zhang, *Chem. Soc. Rev.*, 2013, **42**, 1934–46.
3 Y.-C. Lin, D. O. Dumcenco, Y.-S. Huang and K. Suenaga, *Nat. Nanotechnol.*, 2014, **9**, 391–6.
4 Q. H. Wang, K. Kalantar-Zadeh, A. Kis, J. N. Coleman and M. S. Strano, *Nat. Nanotechnol.*, 2012, **7**, 699–712.
5 M. Xu, T. Liang, M. Shi and H. Chen, *Chem. Rev.*, 2013, **113**, 3766–3798.
6 J. N. Coleman, M. Lotya, A. O'Neill, S. D. Bergin, P. J. King, U. Khan, K. Young, A. Gaucher, S. De, R. J. Smith, I. V Shvets, S. K. Arora, G. Stanton, H.-Y. Kim, K. Lee, G. T. Kim, G. S. Duesberg, T. Hallam, J. J. Boland, J. J. Wang, J. F. Donegan, J. C. Grunlan, G. Moriarty, A. Shmeliov, R. J. Nicholls, J. M. Perkins, E. M. Grieveson, K. Theuwissen, D. W. McComb, P. D. Nellist and V. Nicolosi, *Sci.* , 2011, **331** , 568–571.
7 V. Nicolosi, M. Chhowalla, M. G. Kanatzidis, M. S. Strano and J. N. Coleman, *Sci.* , 2013, **340** .
8 Y. Zhan, Z. Liu, S. Najmaei, P. M. Ajayan and J. Lou, *Small*, 2012, **8**, 966–971.
9 Y. Lee, J. Lee, H. Bark, I.-K. Oh, G. H. Ryu, Z. Lee, H. Kim, J. H. Cho, J.-H. Ahn and C. Lee, *Nanoscale*, 2014, **6**, 2821–2826.
10 Y.-C. Lin, W. Zhang, J.-K. Huang, K.-K. Liu, Y.-H. Lee, C.-T. Liang, C.-W. Chu and L.-J. Li, *Nanoscale*, 2012, **4**, 6637–6641.
11 Y.-H. Lee, X.-Q. Zhang, W. Zhang, M.-T. Chang, C.-T. Lin, K.-D. Chang, Y.-C. Yu, J. T.-W. Wang, C.-S. Chang, L.-J. Li and T.-W. Lin, *Adv. Mater.*, 2012, **24**, 2320–2325.
12 K.-K. Liu, W. Zhang, Y.-H. Lee, Y.-C. Lin, M.-T. Chang, C.-Y. Su, C.-S. Chang, H. Li, Y. Shi, H. Zhang, C.-S. Lai and L.-J. Li, *Nano Lett.*, 2012, **12**, 1538–1544.
13 D. De, J. Manongdo, S. See, V. Zhang, A. Guloy and H. Peng, *Nanotechnology*, 2013, **24**, 25202.
14 H. S. Song, S. L. Li, L. Gao, Y. Xu, K. Ueno, J. Tang, Y. B. Cheng and K. Tsukagoshi, *Nanoscale*, 2013, **5**, 9666–9670.
15 T. S. Pan, D. De, J. Manongdo, A. M. Guloy, V. G. Hadjiev, Y. Lin and H. B. Peng, *Appl. Phys. Lett.*, 2013, **103**, 093108.
16 S. T. Meyers, J. T. Anderson, C. M. Hung, J. Thompson, J. F. Wager and D. A. Keszler, *J. Am. Chem. Soc.*, 2008, **130**, 17603–17609.
17 M.-G. Kim, J. W. Hennek, H. S. Kim, M. G. Kanatzidis, A. Facchetti and T. J. Marks, *J. Am. Chem. Soc.*, 2012, **134**, 11583–11593.
18 K. K. Banger, Y. Yamashita, K. Mori, R. L. Peterson, T. Leedham, J. Rickard and H. Sirringhaus, *Nat. Mater.*, 2011, **10**, 45–50.
19 D. Keszler, *Nat. Mater.*, 2011, **10**, 9–10.
20 D. V Talapin, J.-S. Lee, M. V Kovalenko and E. V Shevchenko, *Chem. Rev.*, 2009, **110**, 389–458.
21 N. G. Deshpande, A. A. Sagade, Y. G. Gudage, C. D. Lokhande and R. Sharma, *J. Alloys Compd.*, 2007, **436**, 421–426.
22 C. D. Lokhande, *J. Phys. D. Appl. Phys.*, 1990, **23**, 1703.
23 T. K. Todorov, O. Gunawan, T. Gokmen and D. B. Mitzi, *Prog. Photovoltaics Res. Appl.*, 2013, **21**, 82–87.
24 W. Liu, D. B. Mitzi, M. Yuan, A. J. Kellock, S. J. Chey and O. Gunawan, *Chem. Mater.*, 2009, **22**, 1010–1014.
25 D. B. Mitzi, M. Copel and C. E. Murray, *Adv. Mater.*, 2006, **18**, 2448–2452.
26 D. B. Mitzi, M. Copel and S. J. Chey, *Adv. Mater.*, 2005, **17**, 1285–1289.
27 D. B. Mitzi, L. L. Kosbar, C. E. Murray, M. Copel and A. Afzali, *Nature*, 2004, **428**, 299–303.
28 J.-S. Lee, M. V Kovalenko, J. Huang, D. S. Chung and D. V Talapin, *Nat. Nanotechnol.*, 2011, **6**, 348–52.
29 D. S. Chung, J.-S. Lee, J. Huang, A. Nag, S. Ithurria and D. V Talapin, *Nano Lett.*, 2012, **12**, 1813–1820.
30 T. K. Todorov, K. B. Reuter and D. B. Mitzi, *Adv. Mater.*, 2010, **22**, E156–E159.
31 D. B. Mitzi, S. Raoux, A. G. Schrott, M. Copel, A. Kellock and J. Jordan-Sweet, *Chem. Mater.*, 2006, **18**, 6278–6282.
32 D. B. Mitzi, *Adv. Mater.*, 2009, **21**, 3141–3158.
33 Z. Jakšić and J. Matovic, *Materials (Basel).*, 2010, **3**, 165–200.
34 H. Li, Z. Yin, Q. He, H. Li, X. Huang, G. Lu, D. W. H. Fam, A. I. Y. Tok, Q. Zhang and H. Zhang, *Small*, 2012, **8**, 63–67.
35 G. S. Armatas and M. G. Kanatzidis, *Nat. Mater.*, 2009, **8**, 217–22.
36 S. Bag and M. G. Kanatzidis, *J. Am. Chem. Soc.*, 2010, **132**, 14951–14959.
37 X. Li, J. Zhu and H. Li, *Appl. Catal. B Environ.*, 2012, **123–124**, 174–181.
38 Y. C. Zhang, J. Li, M. Zhang and D. D. Dionysiou, *Environ. Sci. Technol.*, 2011, **45**, 9324–9331.
39 P. Nørby, J. Overgaard, P. S. Christensen, B. Richter, X. Song, M. Dong, A. Han, J. Skibsted, B. B. Iversen and S. Johnsen, *Chem. Mater.*, 2014, **26**, 4494–4504.
40 M. V Kovalenko, M. I. Bodnarchuk, J. Zaumseil, J.-S. Lee and D. V Talapin, *J. Am. Chem. Soc.*, 2010, **132**, 10085–10092.

41 J. P. Gowers and P. A. Lee, *Solid State Commun.*, 1970, **8**, 1447–1449.
42 S. Singh, M. Festin, W. R. T. Barden, L. Xi, J. T. Francis and P. Kruse, *ACS Nano*, 2008, **2**, 2363–2373.
43 W. A. Woishnis and S. Ebnesajjad, *Chemical resistance of thermoplastics*, William Andrew, Norwich, N.Y., 2012.